ORIGINAL ARTICLE

MUC13 protects colorectal cancer cells from death by activating the NF-κB pathway and is a potential therapeutic target

YH Sheng[1], Y He[2], SZ Hasnain[1], R Wang[1], H Tong[1], DT Clarke[3], R Lourie[1,4], I Oancea[1,4], KY Wong[1], JW Lumley[5], TH Florin[4], P Sutton[6,7,8], JD Hooper[2], NA McMillan[3] and MA McGuckin[1]

MUC13 is a transmembrane mucin glycoprotein that is over produced by many cancers, although its functions are not fully understood. Nuclear factor-κB (NF-κB) is a key transcription factor promoting cancer cell survival, but therapeutically targeting this pathway has proved difficult because NF-κB has pleiotropic functions. Here, we report that MUC13 prevents colorectal cancer cell death by promoting two distinct pathways of NF-kB activation, consequently upregulating BCL-X$_L$. MUC13 promoted tumor necrosis factor (TNF)-induced NF-κB activation by interacting with TNFR1 and the E3 ligase, cIAP1, to increase ubiquitination of RIPK1. MUC13 also promoted genotoxin-induced NF-κB activation by increasing phosphorylation of ATM and SUMOylation of NF-κB essential modulator. Moreover, elevated expression of cytoplasmic MUC13 and NF-κB correlated with colorectal cancer progression and metastases. Our demonstration that MUC13 enhances NF-κB signaling in response to both TNF and DNA-damaging agents provides a new molecular target for specific inhibition of NF-κB activation. As proof of principle, silencing MUC13 sensitized colorectal cancer cells to killing by cytotoxic drugs and inflammatory signals and abolished chemotherapy-induced enrichment of CD133^{+} CD44^{+} cancer stem cells, slowed xenograft growth in mice, and synergized with 5-fluourouracil to induce tumor regression. Therefore, these data indicate that combining chemotherapy and MUC13 antagonism could improve the treatment of metastatic cancers.

Oncogene (2017) 36, 700–713; doi:10.1038/onc.2016.241; published online 11 July 2016

INTRODUCTION

Colorectal cancers are the third most common cause of cancer in men and women. Mortality has been decreasing due to polyp detection–cancer prevention programs, but mortality remains high when colorectal cancer is metastatic. One of the hallmark features of cancers is resistance to apoptotic cell death. Most metastatic cancer therapies act either directly or indirectly via induction of apoptosis in cancer cells,[1] but such therapies are not selective for neoplastic cells.[2] Thus, enhancing selectivity of cancer treatments remains an important chemotherapeutic goal.

Mucins are complex cell surface and secreted glycoproteins that provide protection and lubrication to the epithelial surface of mucosal tissues.[3–5] Aberrant expression of cell surface mucins occurs in many cancers and has been linked to the initiation, progression and poor prognosis of multiple types of adenocarcinoma.[6,7] The advantage of expression in these cancers is likely linked to the normal functions of mucins related to epithelial resistance and resilience to toxic challenges at mucosal surfaces.[4,5] Consequently, mucins are now recognized as potential diagnostic markers and therapeutic targets in many cancers.[8–15]

The MUC13 cell surface mucin is over produced in gastric,[16] colorectal,[17–19] pancreatic[20,21] and ovarian[22] cancers. Normally this protein is synthesized on the apical borders of epithelial cells, including the luminal surface glycocalyx of enterocytes and goblet cells in the small and large intestine,[23] with increased cytoplasmic expression seen in response to infection[24] and inflammation.[25] MUC13 has a 69 amino-acid cytoplasmic domain that includes eight serine and two tyrosine residues for potential phosphorylation, and a protein kinase C consensus phosphorylation motif[23] that could play a critical role in tumorigenesis via cell signaling pathways that regulate apoptosis and proliferation.[18,22,23,25] We have previously shown that MUC13 protects colonic epithelial cells from apoptosis[25] and, therefore, targeting MUC13 and MUC13-regulated pathways to sensitize cancer cells to killing may present an attractive target for cancer treatment.

The intrinsic cell death pathway involves cellular stresses including DNA damage, whereas the extrinsic cell death pathway responds to immune-mediated signals.[26] The nuclear factor-kappa-B (NF-κB) family of transcription factors play a key role in the transcription of several genes involved in the suppression of both cell death pathways.[27] NF-κB signaling networks can be induced by both inflammatory signals (such as tumor necrosis factor-α (TNF-α) and chemotherapy agents). Thus, activation of NF-κB by chemotherapeutic compounds can contribute substantially to the acquired chemo-resistance that hinders effective cancer therapy[28] and promotes recurrence.[29]

In this study, we demonstrate that MUC13 protects human colorectal cancer cells from cell death in response to activation of both intrinsic and extrinsic pathways via NF-κB activation and

subsequent upregulation of the critical regulator of apoptosis, BCL-X$_L$. These *in vitro* data are supported by analysis of patient colorectal cancers which showed a correlation between cytoplasmic MUC13 expression, tumor grade, and expression of NF-κB proteins and BCL-X$_L$. Importantly, in human tumor cell line xenograft models, *MUC13* siRNA treatment reduced the growth of colorectal cancers and synergized with 5-fluorouracil (5-FU) to induce regression of established tumors.

RESULTS

MUC13 is required for survival and growth of colorectal cancer cells

To assess the effects of endogenous MUC13 on the sensitivity of human cancer cells to death, we used three colorectal cancer cell lines—LS513, LIM2463 and HT29. LS513 and LIM2463 cells have high MUC13 expression and harbor inactivating mutations in the tumor suppressors *APC* and *TP53*, and activating mutations in the oncogenes encoding PIK3CA and KRAS (features frequently observed in colorectal cancers), whereas HT29 cells have inactivating mutations in *TP53*, but are KRAS wild type with moderate MUC13 expression. We first knocked down *MUC13* with siRNA in these cell lines, and then treated them with TNF and cycloheximide (which sensitizes cells to TNF-induced apoptosis by blocking synthesis of antiapoptotic proteins) and cell survival was determined by measuring ATP levels. *MUC13* siRNA reduced MUC13 protein expression by ~ 80% in these cell lines (Supplementary Figure S1A) and resulted in a significant decrease in cell survival following cycloheximide treatment alone in LS513 and LIM2463 cells, and after TNF/cycloheximide co-treatment in LS513, LIM2463 and HT29 cells, when compared with control siRNA (Figure 1a). TNF treatment alone did not induce cell death, but conversely increased cell number in control cells, but not in *MUC13*-silenced cells (Figure 1a). Consistent with this observation, we found that silencing *MUC13* also increased cell death following actinomycin D, ultraviolet radiation or TNF-related apoptosis-inducing ligand (TRAIL) exposure, compared with control siRNA, in the LS513 and LIM2463 cell lines, as evidenced by the large increase in numbers of both Annexin-V$^+$/7ADD$^-$ and Annexin-V$^+$/7ADD$^+$ cells (Figures 1b and c and Supplementary Figures S1B and C). These data support MUC13's role as an important pro-survival factor in colorectal cancer.

We also demonstrated that MUC13 promotes cell proliferation by measuring cell growth in real time using a xCELLigence impedence analyser (ACEA Biosciences, San Diego, CA, USA), with MUC13-silenced LS513, LIM2463 and HT29 cells showing slower proliferation than control siRNA-treated cells (Supplementary Figure S1D). Further supporting a pro-survival role for MUC13, its overexpression in SW480 colon cancer cells (Supplementary Figure S1E) protected these cells from TNF/cycloheximide-induced death (Figure 1d) and enhanced their proliferation vs vector-transfected control cells (Supplementary Figure S1F).

MUC13 increases expression of BCL-X$_L$ through NF-κB p65 signaling

To investigate the mechanism by which MUC13 promotes cell survival, we examined expression of critical regulators of apoptosis, the BCL2 family of genes.[30] Silencing of *MUC13* significantly decreased mRNA expression of the antiapoptotic genes *BCL2L1* (encodes BCL-X$_L$), but not *BCL2* (encodes BCL2), and increased expression of the proapoptotic gene *BCL2L11* (encodes BIM) (Figure 2a). Decreased expression of MUC13 significantly reduced protein levels of BCL-X$_L$ consistent with mRNA analysis, but did not change protein levels of BIM (Figure 2b), indicating that a potential mechanism by which MUC13 protects cancer cells from cell death is by upregulation of BCL-X$_L$. In support of BCL-X$_L$ being an active suppressor of cell death in these cells and a downstream mediator of MUC13's protective role, in the presence of the functional

inhibitor of BCL-X$_L$, ABT-263, TNF/cycloheximide-induced equivalent high amounts of cell death in control siRNA- and *MUC13* siRNA-treated cells (Figure 2c).

BCL-X$_L$ is known to be regulated by NF-κB RelA (p65) signaling in epithelial cells.[31] Therefore we used a panel of inhibitors to address whether the regulation of BCL-X$_L$ expression by MUC13 is dependent on this pathway. Western blotting demonstrated that the NF-κB inhibitor, Bay 11-7085, decreased mean BCL-X$_L$ protein levels by ~ 37% and eliminated the difference in protein levels caused by *MUC13*-silencing (Figure 2d and Supplementary Figure S2). To determine whether MUC13 affects the NF-κB transcription complex, we performed chromatin immuno-precipitation (Chip) assays with anti-p65 antibody. Chip of the NF-κB responsive element in the promoter of the BCL-X$_L$ gene was analyzed by semiquantitative PCR. In LS513 cells, in the absence of any inflammatory stimuli, the NF-κB responsive element of the BCL-X$_L$ promoter was occupied by p65 and occupation was eliminated by silencing *MUC13* (Figure 2e). As a control, there was no detectable signal in Chip's performed with non-immune IgG (Figure 2e). These data suggested that MUC13 upregulated BCL-X$_L$ expression through NF-κB signaling in colorectal cancer cell lines.

MUC13 and BCL-X$_L$ are concomitantly increased in primary colorectal cancer

To examine the relevance of our *in vitro* findings to colorectal cancer in patients, we assessed the expression of MUC13 and BCL-X$_L$ in lysates from matched non-diseased and malignant colon tissue. In this series of 29 colon cancers and adjacent uninvolved colonic tissue, MUC13 protein levels were greater in 82% of tumors compared with adjacent non-diseased tissue (Figure 3a). Furthermore, there was a significant correlation between MUC13 and BCL-X$_L$ protein levels in tumors but not in non-diseased tissues (Figure 3b), further strengthening the potential functional link between these proteins *in vivo*. Interestingly, we also observed relatively low levels of TNFR1 in human colorectal cancer and colorectal cancer cell lines (Supplementary Figures S3A and B).

Cytoplasmic MUC13 expression increases in high grade and metastatic colorectal cancer and correlates with expression of NF-κB and BCL-X$_L$

To explore the relationship between expression of MUC13 and tumor grade and metastasis, we assessed MUC13 staining in colorectal cancers from 192 patients by immunohistochemistry. Colon tissues presented different degrees of immunoreactive scores for MUC13 and different patterns of cellular staining (Supplementary Figures S3C and D). Of the 192 specimens, 89% of tumors presented with high (immunoreactive scores > 4) and 11% with low (immunoreactive scores ⩽ 4) MUC13 protein. Normal tissue showed weak MUC13 staining, which was largely restricted to the apical surface of cells but membrane staining was increased in low-grade tumors (Supplementary Figures S3C and D). In high-grade cancer, there was more frequent strong cytoplasmic staining of MUC13, whereas apical cell surface staining of MUC13 decreased with advanced histological grade (Supplementary Figures S3C and D). A small proportion of tumors showed nuclear staining of MUC13, typically in a small proportion of tumor cells.

We also investigated cytoplasmic MUC13 staining in colorectal cancer progression using a tissue array that contained normal colon tissue, benign tumors, and primary and metastatic colorectal cancers. There was significantly increased cytoplasmic MUC13 in primary colon tumors and lymph node metastases, compared with normal tissue and benign tumors (Figure 3c). Given our *in vitro* findings that MUC13 upregulated BCL-X$_L$ expression in colorectal cancer cell lines through NF-κB signaling, we also evaluated NF-κB p65 staining by immunohistochemistry, and observed that immunoreactive scores of NF-κB showed a similar trend to MUC13 with increasing scores with colorectal cancer progression (Figure 3c). Importantly, the expression
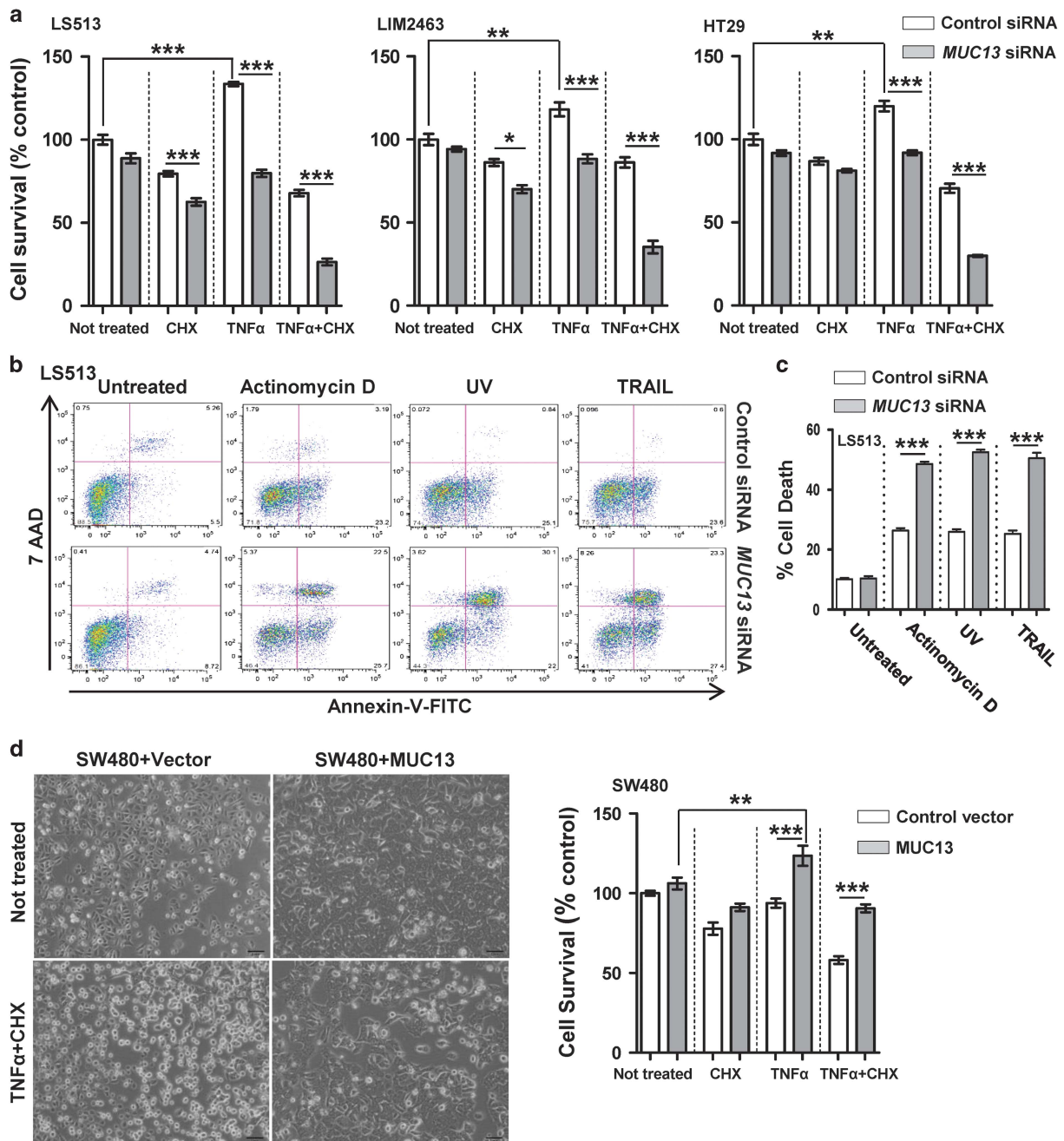
Figure 1. MUC13 protects colorectal cancer cells from intrinsic and extrinsic cell death-inducing agents and promotes proliferation. The indicated CRC cells were transfected with *MUC13* or control siRNA for 48 h, and then treated for a further 15 h with either (**a**) cycloheximide (CHX) (4 μg/ml for both LS513 and LIM2463 cells, 8 μg/ml for HT29 cells) and/or TNF (25 ng/ml) or (**b**, **c**) actinomycin D (1 μM), UV (60 mJ/cm^3) and TRAIL (40 μg/ml). (**a**) Live cell activity in the cultures was determined by measuring ATP levels and expressed as % of cells treated with control siRNA and vehicle control. (**b**) Representative flow cytometry plots of cells stained with Annexin-V/7-AAD. (**c**) The percentage of cell death in Annexin-V$^+$ and/or 7-AAD$^+$ cells determined by flow cytometry. (**d**) Control and MUC13-overexpressing SW480 cells were treated with CHX (8 μg/ml) and/or TNF (25 ng/ml) for 15 h. Photomicrographs after treatment (scale bar, 200 μм) and cell survival (determined by measuring ATP levels as in (**a**)) are shown. A representative of three independent experiments is shown as mean ± s.e.m., $n = 4$. One-way ANOVA with Tukey *post hoc* test; ***P < 0.0001, **P < 0.001, *P < 0.05. See Supplementary Figure S1 for verification of MUC13 silencing and transfection, and for analysis of proliferation in the indicated CRC cells and apoptosis in LIM2463 cells.

of MUC13 significantly correlated with expression of NF-κB in primary cancers and particularly in lymph node metastases (Figure 3d). Taken together, these data are consistent with the mechanism we described *in vitro* whereby MUC13 enhances NF-κB-mediated expression of BCL-X$_L$. Importantly, our demonstration that elevated expression of cytoplasmic MUC13 and NF-κB correlated with tumor progression and metastases in cancer patients provides a new

molecular target for inhibiting NF-κB activation more specifically in advanced colorectal cancers.

TNF-induced activation of the NF-κB pathway is impaired in MUC13-deficient cells
Given our findings of differential responses to TNF in *MUC13*-silenced cells, and MUC13 promotion of NF-κB p65 activation of
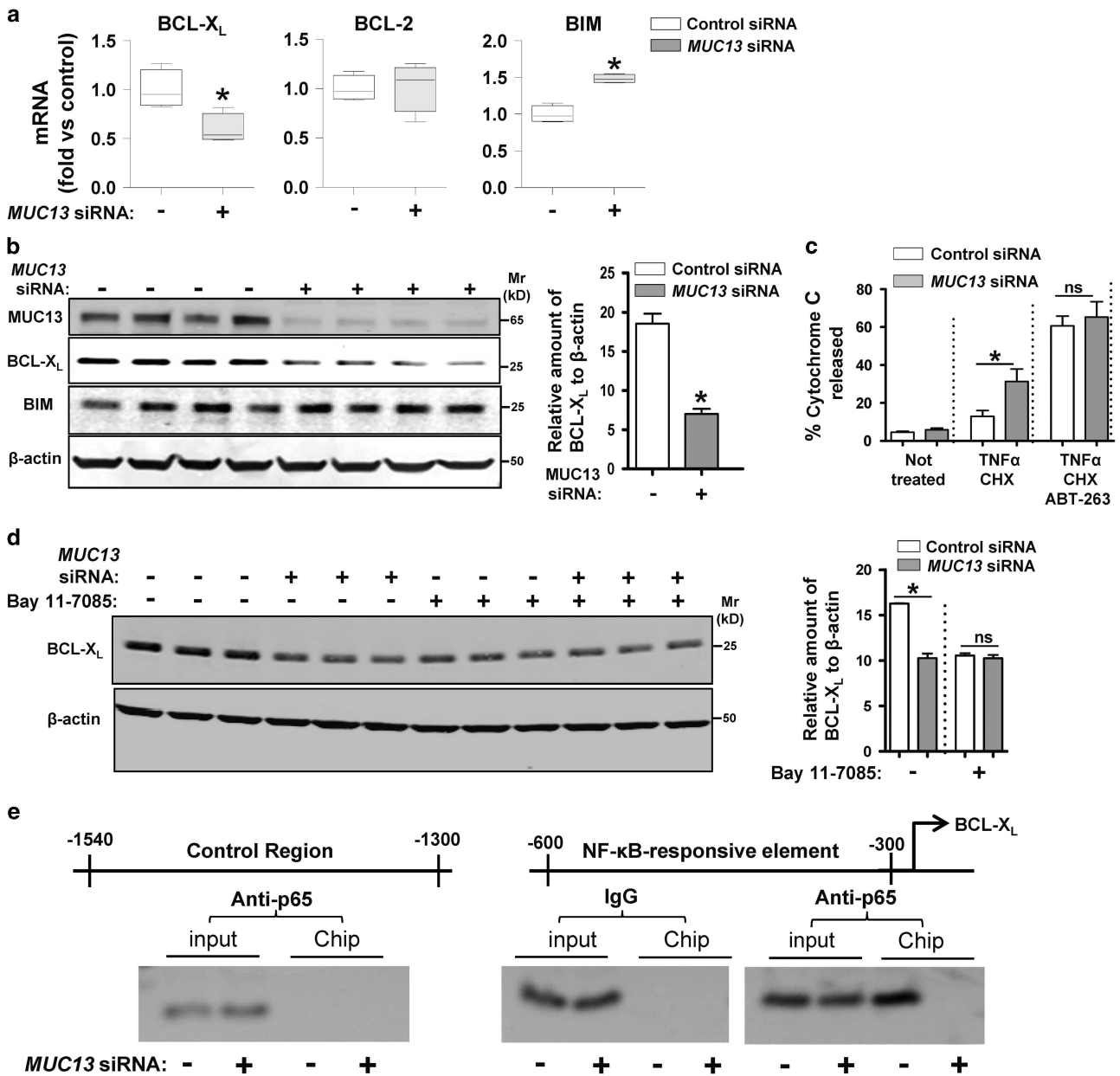
Figure 2. MUC13 increases expression of BCL-X$_L$ by enhancing NF-κB p65-mediated transcription. Treatment of LS513 cells with *MUC13* siRNA decreased BCL-X$_L$ protein levels. (**a**) Relative *BCL2L1* (BCL-X$_L$), *BCL2* (BCL2) and *BCL2L11* (BIM) mRNA levels (corrected for β-actin) in LS513 cells. (**b**) The level of BCL-X$_L$ and BIM proteins in LS513 cells; densitometry analysis of BCL-X$_L$ corrected for β-actin is shown in the right panel. (**c**) Cell death was determined by a cytochrome-*c* release flow cytometry assay after 15 h exposure to CHX (4 μg/ml) plus TNF (25 ng/ml) with or without the BCL-X$_L$ inhibitor ABT-263 (1 μM). (**d**) Cells treated with pharmacological inhibitors of NF-κB (Bay 11-7085 (Bay), 5 μM) for 24 h and immunoblotted with BCL-X$_L$ and β-actin antibodies and analyzed as in (**b**). (**e**) Soluble chromatin extracted from LS513 cells transfected with control or *MUC13* siRNA was immunoprecipitated with anti-p65 antibody or a control IgG. DNA extracted from immunoprecipitates was amplified by PCR with pairs of primers that cover the NF-κB-response element (−600 to −300) or a control region (CR; −1540 to −1300) in the BCL-X$_L$ promoter. A representative of three independent experiments is shown as mean ± s.e.m., $n = 4$ (**b**, **c**), $n = 3$ (**d**). Mann–Whitney *U*-test, vs control siRNA with same treatment; *$P < 0.05$. See Supplementary Figure S2 for the effect of other pathway inhibitors on BCL-X$_L$ expression.

a downstream target gene,[32] we examined whether NF-κB activation in response to TNF was compromised in the absence of MUC13. Indeed, phosphorylation of p65 upon TNF treatment was substantially impaired in *MUC13*-silenced LS513 cells (Figure 4a). Interestingly, the individual cells that remained TNF-responsive were those that still expressed detectable MUC13 despite siRNA transfection.

Based on these findings, the question emerged of how MUC13 is biochemically linked to the promotion of NF-κB activation. MUC1 has been shown to drive constitutive activation of

NF-κB in human carcinoma cells by interacting directly with IKKβ and NF-κB essential modulator (NEMO).[33,34] Since it is possible that this is a conserved mechanism shared by all cell surface mucins, we examined for interactions of MUC13 with NF-κB proteins by co-immunoprecipitation. However, we could not demonstrate interactions between MUC13 and IKKα, IKKβ, NEMO, or p65 (Supplementary Figure S4A).

Because MUC13 deficiency caused defects in TNF-induced NF-κB signaling, we next explored the possibility that MUC13 might act upstream of NF-κB as a component of the complex involving
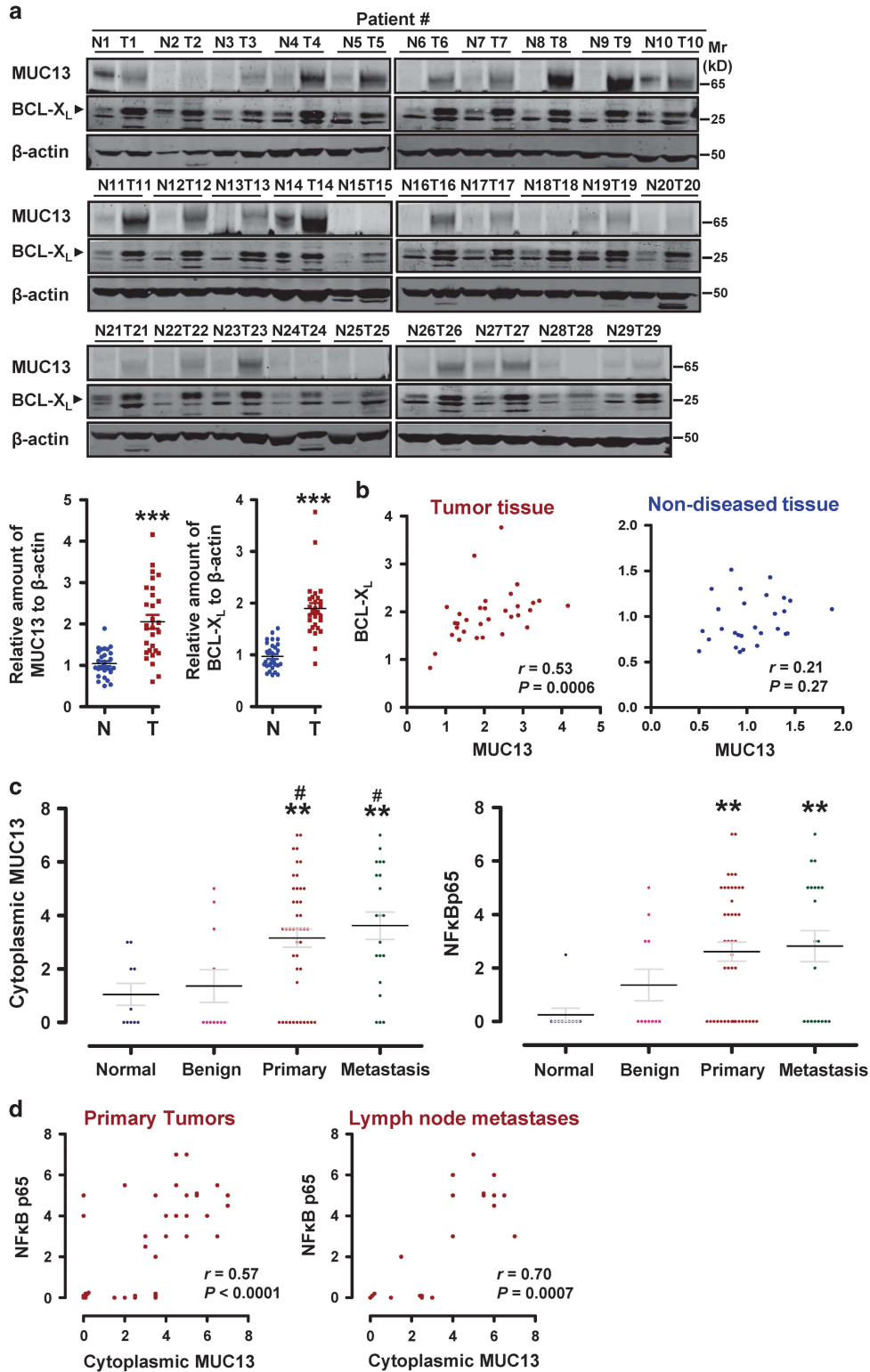
Figure 3. Cytoplasmic MUC13 increases in metastatic colon cancer and correlates with staining for NF-κB and BCL-X$_L$. (**a**) Western blots and densitometry analysis showing expression of MUC13 and BCL-X$_L$ in primary CRC (T) and non-diseased colon tissue (N). (**b**) Correlation plot of MUC13 and BCL-X$_L$ expression in CRC and non-diseased colon tissue. (**c**) Cytoplasmic MUC13 protein levels and NF-κB p65 protein levels in a distinct tissue microarray with samples from various stages of colon cancer progression which included 10 non-diseased colon tissues, 11 benign tumors, 46 primary CRC and 20 CRC lymph node metastases. (**d**) Correlation plots of cytoplasmic MUC13 and NF-κB expression in primary tumors and lymph nodes metastases. Statistics: (**a**, **c**) mean ± s.e.m. Mann–Whitney *U*-test, * vs normal tissue, # vs benign tumor; *[#]*$P < 0.05$, **$P < 0.001$. See Supplementary Figure S3 for TNFR1 expression in the matched primary tumor and normal tissues from (**a**) and for analysis of cytoplasmic MUC13 expression vs cancer grade.

the TNF receptor. Co-immunoprecipitation experiments demonstrated that MUC13 co-precipitates with TNFR1 and the E3 ubiquitin ligase, cIAP1, and that this association occurs in both unstimulated and TNF-stimulated LS513 and HT29 cells (Figure 4b). The specificities of these interactions were confirmed by reverse immunoprecipitation of MUC13 (Figure 4b). This indicates that MUC13 interacts with the complex involving TNFR1 and cIAP1 in both unstimulated and TNF-stimulated colorectal cancer cell lines.

TNF stimulation generates two distinct signaling complexes, one dedicated to NF-κB activation resulting in cell survival and the other for cell death.[35] The NF-κB activation cascade is a paradigm for the role of RIPK1 ubiquitination in regulating signaling pathways, with RIPK1 ubiquitination contributing to NF-κB signaling.[35,36] The defect in NF-κB activation in MUC13-silenced cells, together with the discovery that MUC13 interacts with cIAP1 E3 ligase, suggested that MUC13 may enhance ubiquitination of RIPK1. Therefore, we investigated the ubiquitination of RIPK1 in cells deficient in MUC13 and also in cells stably overexpressing MUC13. Transient knockdown of MUC13 in LS513 cells reduced the K63-linked ubiquitination of RIPK1 in response to TNF (Figure 4c). Conversely, overexpression of MUC13 in SW480 cells increased TNF-stimulated K63-linked ubiquitination of RIPK1 (Figure 4c). Given the change in ubiquitinated RIPK1 and because NEMO is an important partner for RIPK1 in NF-κB signaling,[36] we next examined the ability of RIPK1 and NEMO to interact in the presence and absence of MUC13. This showed that more NEMO, as well as more cIAP1 and TRAF6, associated with RIPK1 in MUC13-expressing, as compared with MUC13 deficient, LS513 cells stimulated with TNF (Figure 4d). Increased co-precipitation occurred despite similar total levels of NEMO, cIAP1 and TRAF6 proteins in MUC13-expressing and MUC13-deficient LS513 cells (Supplementary Figure S4B).

To determine the effect of MUC13 depletion on TNF-induced NF-κB-regulated transcription in colorectal cancer cells, we examined the expression of a panel of NF-κB-regulated genes. In line with impaired phosphorylation of p65 (Figure 4a), upon TNF treatment overall expression of the NF-κB target genes were significantly reduced in MUC13 siRNA-treated LS513 and LIM2463 cells (Figure 4e and Supplementary Figure S4C). These experiments suggest that MUC13 enhances recruitment of cIAP1 to the TNFR/RIPK1 complex, and that the cIAP1 E3 ubiquitin ligase promotes K63-linked ubiquitination of RIPK1 and in turn, activation of NF-κB and downstream NF-κB-regulated gene expression.

MUC13 is also required for activation of NF-κB in response to DNA damage

As MUC13 also protected cells from cell death in response to UV radiation, we also addressed whether NF-κB activation by DNA-damaging agents might also be compromised in the absence of MUC13. After etoposide treatment nuclear translocation of NF-κB p65 (detected with either phosphorylation-independent or phospho-Ser536 antibody) was significantly impaired in MUC13-silenced LS513 and LIM2463 cells (Figure 5a). As the activation of the kinase ATM and modifications of NEMO have important roles in the activation of NF-κB in response to genotoxic stress,[37] we investigated the influence of MUC13 on activation (phosphorylation) of ATM and SUMOylation of NEMO in response to DNA-damaging agents. Although MUC13 did not influence total cellular ATM levels, ATM activation was impaired in MUC13 siRNA-treated LS513 cells upon etoposide treatment (Figure 5b). As expected, etoposide lead to a decrease in total IκBα accompanied by its phosphorylation, whereas total IκBα did not diminish and phosphorylation of IκBα was reduced in MUC13-siRNA-treated cells. These changes in IκBα are likely to be a direct consequence of reduced ATM phosphorylation (Figure 5b). Furthermore, knockdown of endogenous MUC13 in LS513 cells led to a substantial inhibition of expression of PARP1 (Figure 5b). As a result, SUMOylation of NEMO, which is known to be driven by PARP1, was reduced in

MUC13-deficient cells in response to etoposide (Figure 5c). Interestingly, MUC13 depletion also substantially reduced the ubiquitination of RIPK1 in response to etoposide in a similar manner as in response to TNF and cycloheximide (Figure 5d).

Silencing MUC13 increases chemotherapy-induced DNA damage in vitro

We next investigated if treatment with MUC13 siRNA could be used to sensitize colorectal cancer cells to DNA-damaging chemotherapeutic drugs. The IC_{50} of MUC13-silenced cells to four drugs with differing mechanisms of action that result in DNA damage (5-fluorouracil, vincristine, oxaliplatin and doxorubicin) was 3- to 19-fold less in LS513 cells, and 2- to 26-fold less in LIM2463 cells, than in control siRNA-treated cells (Figure 5e). Overall, these data and those described earlier show that MUC13 prevents cancer cell death by promoting two distinct signaling pathways to NF-κB activation, inhibiting the intrinsic and extrinsic cell death pathways and thereby promoting cancer cell survival.

## MUC13 silencing in vivo slows growth and sensitizes tumors to chemotherapy

Having established the importance of MUC13 in protecting colorectal cancer cells from death in vitro, we next examined chemosensitisation in vivo. Initially, LS513 subcutaneous xenografts established in NOD/SCID gamma mice were treated 3, 5, 7 and 10 days following tumor cell inoculation with liposomes containing 40 μg of either MUC13 or control siRNA.[38] The four MUC13 siRNA liposome treatments substantially reduced MUC13 protein expression in the LS513 tumors (sampled one day following the final MUC13 siRNA liposome treatment) (Figure 6a) and delayed tumor growth. At the end of experiments, the mean tumor volume and weight of the MUC13 siRNA-treated group were reduced by >50% compared with controls (Figure 6b).

Significantly, combination of inhibition of MUC13 expression and 5-FU chemotherapy enhanced tumor regression in both KRAS mutant (LS513) and KRAS wild-type (HT29) colorectal cancer xenografts. In these experiments, xenografts were allowed to establish until the average tumor volume was 100–200 mm³ prior to the commencement of 5-FU and siRNA liposome therapy. The dose of 5-FU (50 mg/kg) was chosen based on acceptable toxicity and substantial antitumor activity. MUC13 siRNA treatment alone slowed tumor growth relative to vehicle-treated control in both xenografts (Figures 6c and d). 5-FU (plus control siRNA) also slowed tumor growth, being equally as effective as MUC13 siRNA in LS513 xenografts and slightly more effective in HT29 xenografts (Figures 6c and d). Importantly, combining MUC13 siRNA with 5-FU led to tumor regression in LS513 xenografts and substantially attenuated tumor growth in HT29 xenografts (Figures 6c and d). At the end of the experiment the mean weight of LS513 xenografts treated with MUC13 siRNA or 5-FU alone or the MUC13 siRNA/5-FU combination were 46, 30 and 8%, respectively, of xenografts treated with control siRNA only (Figure 6c). For HT29 xenografts mean tumor weights for MUC13 siRNA or 5-FU alone or in combination were 53, 33 and 18%, respectively, of controls (Figure 6d). Mice tolerated the combined treatment well with no overt signs of toxicity, and white blood cell concentrations declined in 5-FU-treated but not MUC13 siRNA-treated mice (Supplementary Figures S5A and B).

To further explore the mechanism of action of MUC13 silencing in vivo, we quantified the numbers of proliferating (BrdU⁺) and apoptotic (TUNEL⁺) cancer cells in the LS513 tumors sampled at the end of these experiments. MUC13 siRNA liposome/5-FU treatment led to significantly reduced proliferation and increased death of tumor cells (Figure 7a and Supplementary Figure S5C), consistent with the reduction in tumor mass observed with this therapy. MUC13 siRNA liposome or 5-FU treatment alone showed a reduced number of BrdU⁺ cells and an increase in TUNEL⁺ cancer cells, but to a lesser degree than in tumors from

the combined treated group (Figure 7a). In line with our in vitro findings, downregulation of MUC13 by MUC13 siRNA liposome treatment reduced total NF-κB p65 protein and its phosphorylation, and reduced BCL-X$_L$ expression in tumor cells in vivo (Figure 7b). Consistent with engagement of DNA damage survival signaling, we also observed that 5-FU treatment increased the relative amount phosphorylated NF-κB p65 vs its total amount in vivo measured by western blotting (Figure 7b) and the total amount of phosphorylated NF-κB p65 in vitro measured by alphascreen assay (Figure 7c), as previously described,[39] but not
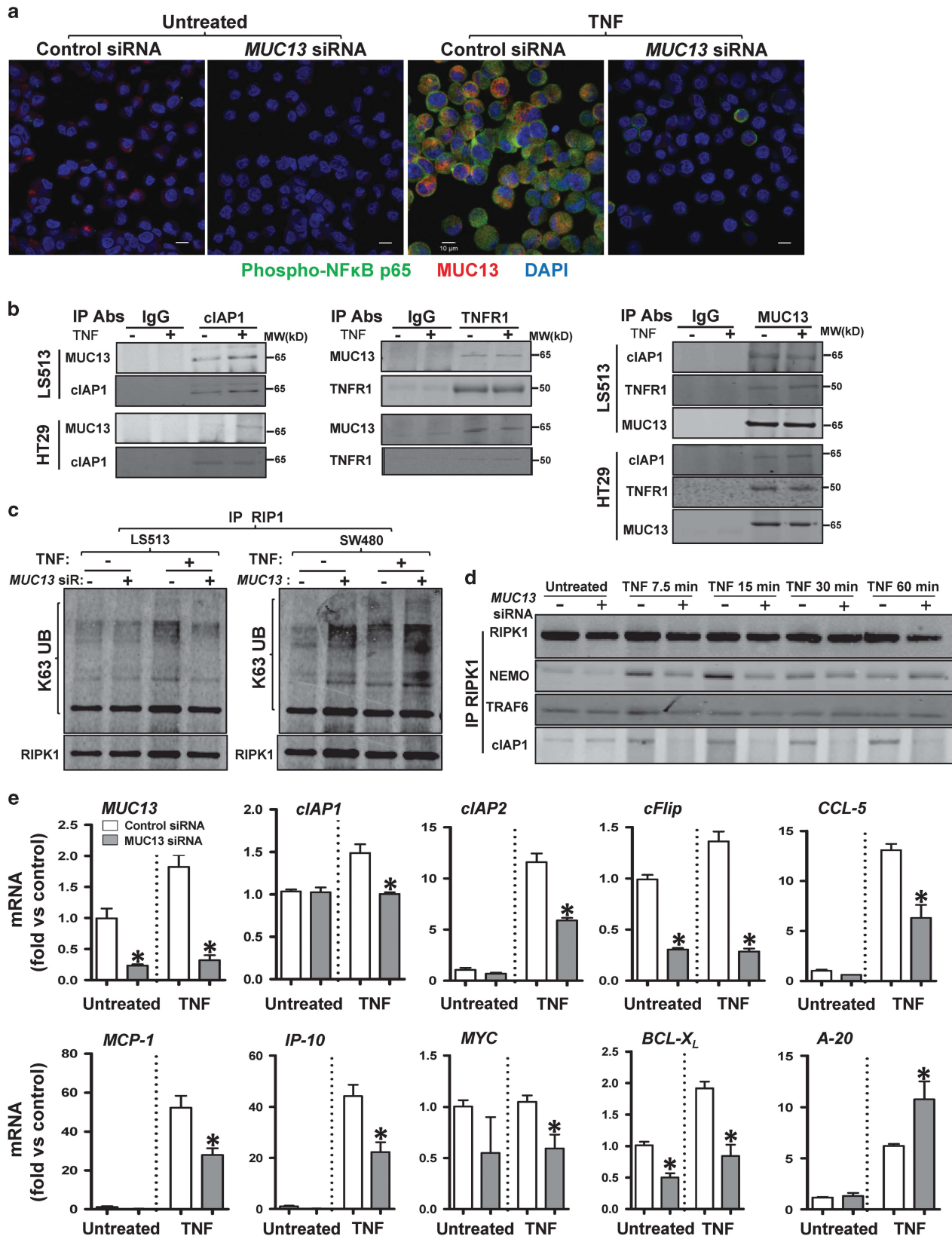
when *MUC13* was silenced (Figures 7b and c). To further extend these findings, we determined whether NF-κB inhibition restores chemosensitivity to 5-FU in MUC13-expressing colorectal cancer cells. LS513 cells were treated with 5-FU with or without the NF-κB inhibitor, Bay 11-7085 (Bay), which alone had no effect on viability under basal conditions but which increased 5-FU-induced cell death in MUC13-expressing cells to the levels seen in MUC13-deficient cells with or without the NF-κB inhibitor (Figure 7d). These results taken together confirm that MUC13 silencing increases sensitivity to 5-FU by removing MUC13-mediated promotion of the NF-κB pathway.

We also examined whether MUC13 expression affected the CD133^{+}/CD44^{+} cancer stem cell (CSC) population in LS513 colorectal cancer cells. This is because studies of CSC have indicated that cancer chemotherapy treatment failure may often be due to the persistence of chemotherapy-resistant CSC.[40] In the normal intestine MUC13 is expressed in the crypt stem cell niche (Supplementary Figure S5D) and the mRNA levels of LGR5 and ALDH1, which are stem cell markers, were significantly lower in MUC13-silenced colorectal cancer cells (Figure 7e). Knockdown of *MUC13* reduced the relative abundance of the CD133^{+}/CD44^{+} population (Figure 7f), and importantly, diminished the enrichment of CSC that occurs following 5-FU treatment (Figure 7f). In contrast, in MUC13-expressing cells 5-FU treatment substantially increased the frequency CD133^{+}/CD44^{+} of CSC in a dose-dependent manner (Figure 7f). These differences in CSC survival between MUC13-expressing and deficient cells indicate that the synergistic actions of *MUC13* siRNA/5-FU *in vivo* may be be partly due to MUC13-mediated protection of CSC cells.

DISCUSSION

While chemotherapy is the mainstay of cancer therapy, limited efficacy and development of resistance to chemotherapeutic drug treatments are major challenges in treatment of epithelial cancers, including metastatic colorectal cancers. Sensitizing cancer cells to chemotherapy in a manner safe to normal tissues is an important therapeutic goal. The identification of new molecular targets is essential to improve outcomes and sensitize cancers to therapy. Moreover, a better understanding of the mechanisms through which the new targets exert their effects is essential to improve combination therapies. Herein, we have identified and characterized MUC13 as a potential therapeutic target for colorectal cancers and shown that antagonizing MUC13 chemo-sensitizes the cancer cells. Our study provides the first empirical evidence that MUC13 plays a critical role in cancer cell resistance to cell death in response to a broad range of therapies by activating the NF-κB survival pathway. We provide several important new insights into the MUC13 regulation of cell survival under stress.

First, our data demonstrate that silencing of MUC13 not only sensitized colon cancer cells to death in response to a wide range of genotoxic drugs *in vitro* but also suppressed tumor growth *in vivo*. Second, our study reveals the major mechanisms by which MUC13 inhibits cell death. MUC13 inhibits both the extrinsic and intrinsic cell death pathways by modulating expression of antiapoptotic genes and pro-survival genes via promotion of NF-κB activation and transcription of downstream target genes (Figure 8). In terms of the extrinsic cell death pathway, we propose that binding of MUC13 to TNFR1 increases clustering of the TNFR1 signaling complex, thereby amplifying the efficiency of TNF-induced signaling given that human colorectal cancers and some colorectal cancer cell lines aberrantly overexpress MUC13 while exhibiting low expression of TNFR1 (Figure 3a and Supplementary Figures S3A and B). In the context of the intrinsic cell death pathway, MUC13 is also required in colonic cells for activation of NF-κB. DNA-damaging agents induce MUC13 cytoplasmic and nuclear translocation and/or retention, allowing MUC13 to accumulate in the cytosol or nucleus where MUC13 promotes phosphorylation of ATM. SUMOylation of NEMO is greater in the presence of MUC13, potentially explained by increased expression of PARP1 which is a DNA damage sensor and catalyses the formation of polyADP-ribose on target substrates, including on PARP1 itself.[41] Auto-modified PARP1 promotes NEMO SUMOylation in the nucleus by assembling a signaling complex. Given that MUC13 interacts with cIAP1, MUC13 may recruit cIAP1 or other E3 ligases to NEMO, leading to its enhanced ubiquitination. As a consequence, ubiquitination of NEMO and activation of ATM ultimately leads to activation of IKKs and NF-κB to promote cell survival. MUC13's presence in the TNFR complex and modulation of TNFR signaling demonstrates function of MUC13 at the cell surface and/or in the cytoplasm following internalization of activated TNFR. At this stage we cannot determine whether the interaction with the TNFR1 complex is mediated by the MUC13 cytoplasmic domain, extracellular domain, or both. Furthermore, while the translocation of MUC13 into the nucleus and association with proteins involved in DNA damage repair suggests a functional role for MUC13 in the nucleus, we do not have direct evidence for this.

Third, we demonstrate that MUC13 protein is highly expressed in primary human colorectal cancers and correlates with BCL-X$_L$ and NF-κB, suggesting that mechanisms detected in cultured cells, such as MUC13 regulation of BCL-X$_L$ via NF-κB activation, are operational in colorectal cancers. Gupta *et al.*[19] have reported high cytoplasmic MUC13 expression in liver metastasis together with a correlation between high cytoplasmic expression and poor differentiation. In addition to confirming that increased cytoplasmic MUC13 expression is significantly associated with tumor grade, we show it is associated with lymph node metastasis and correlates with NF-κB expression in these metastases. Given that the MUC13/NF-κB/BCL-X$_L$ pathway remains in an activated state in colorectal cancer, it was logical that our subsequent studies then demonstrated that inhibiting MUC13 had a therapeutic benefit in colorectal cancer xenografts. Targeting MUC13 to inhibit NF-κB activation to enhance chemospecificity for the tumor appears to offer advantages over more direct inhibition of NF-κB, because most NF-κB inhibitors to date have been disappointing for the treatment of epithelial cancers due to off-target toxicity, with the inhibition of upstream activators showing more promise.[42,43] Potential toxicity of targeting MUC13 needs to be considered and

Figure 4. MUC13 promotes TNF-stimulated activation of the NF-κB signaling pathway by interacting with the TNF-receptor signaling complex and induction of antiapoptotic and inflammatory genes. (**a**) Stimulation of MUC13-expressing cells (red) with TNF (25 ng/ml) for 15 min, but not *MUC13* siRNA-treated cells, induces phosphorylated NF-κB p65 (green). Fluorescence was detected using confocal microscopy. Scale bar, 10 μm. (**b**) LS513 and HT29 cells were treated with TNF (25 ng/ml) for 15 min, then lysates were immunoprecipitated with cIAP1, TNFR1 or MUC13 antibodies, and then subjected to PAGE and western blotted with the indicated antibodies to show co-immunoprecipitation. (**c**) LS513 *MUC13* siRNA-treated cells or SW480 *MUC13*-overexpressing cells were treated with TNF (25 ng/ml) for 15 min, lysed and immunoprecipitated with RIPK1 antibody and western blotted with anti-K63-specific ubiquitin or RIPK1 antibody. (**d**) Kinetic analysis of recruitment of signaling molecules to RIPK1. LS513 cells were transfected with *MUC13* or control siRNA for 48 h, and then treated with TNF (25 ng/ml) for the indicated times, then lysed and immunoprecipitated with RIPK1 antibody and western blotted with the indicated antibodies. (**e**) Relative expression levels of known NF-κB-regulated genes in LS513 *MUC13* siRNA-treated cells. mRNAs were isolated 2 h post stimulation with TNF (25 ng/ml) and analyzed by Q-RT–PCR. All data are representative of three independent experiments. Statistics: (**e**) mean ± s.e.m., $n = 4$. Mann–Whitney *U*-test, vs control siRNA with same treatment; *$P < 0.05$. See Supplementary Figure S4 for co-IP of MUC13 with NF-κB components, expression of TRAF6, cIAP1 and NEMO following TNF stimulation, and altered expression of NF-κB target genes in LIM2463 cells treated as in (**e**).
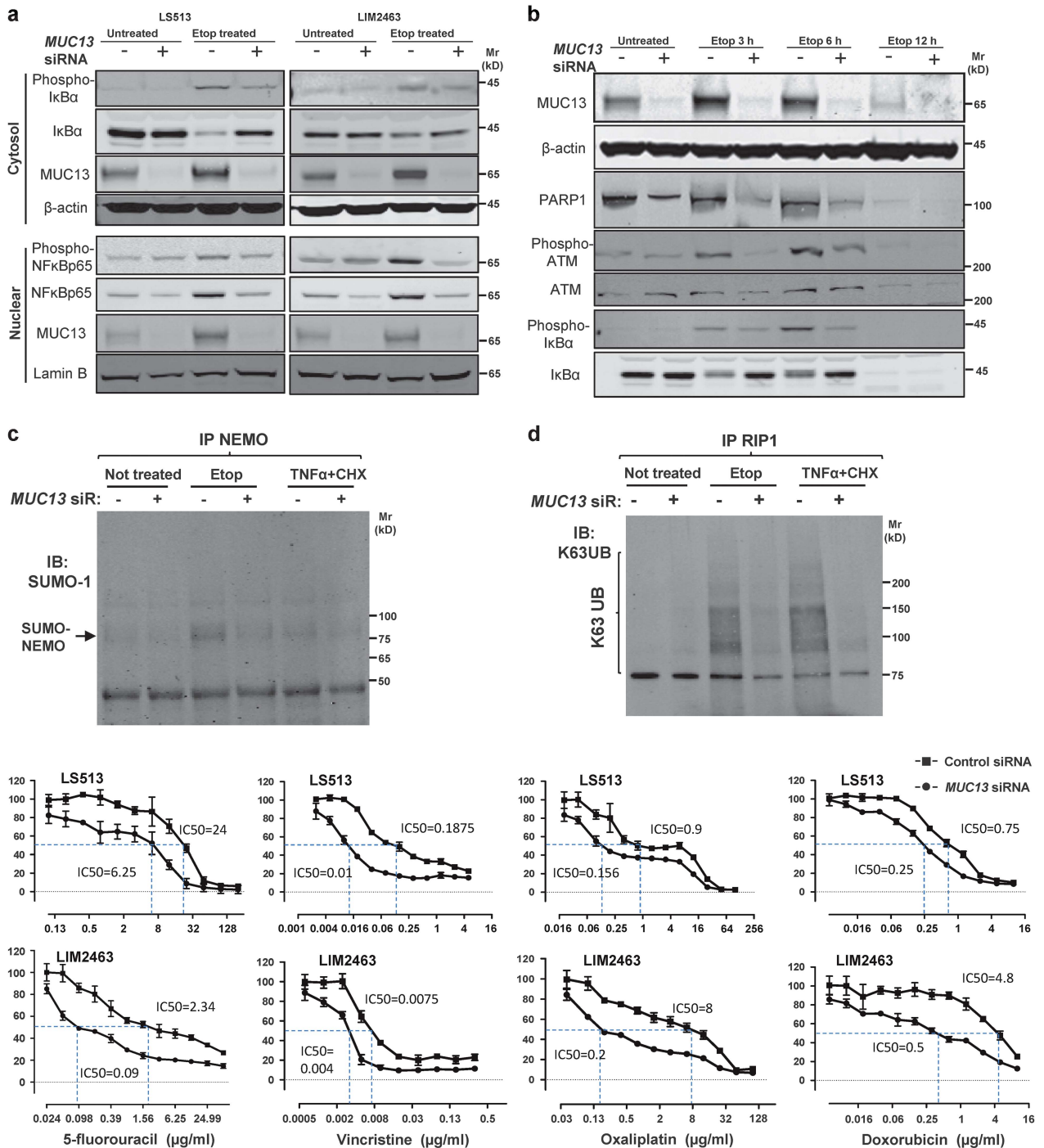
Figure 5. DNA damage triggers MUC13-mediated phosphorylation of ATM and sumolyation of NEMO to activate NF-κB signaling. (**a**) LS513 and LIM2463 cells were transfected with *MUC13* or control siRNA for 48 h and treated with 100 μM etoposide (Etop) for 6 h and cytosolic or nuclear extracts were analyzed by PAGE and immunoblotted with the indicated antibodies to monitor NF-κB activation. (**b**) LS513 cells were transfected as in (**a**) and treated with 100 μM etoposide for the indicated times and whole-cell extracts were analyzed by immunoblotting with the indicated antibodies to monitor PARP1, ATM phosphorylation and NF-κB activation. (**c**) LS513 cells were transfected as in (**a**), and then treated with either 100 μM etoposide for 6 h or TNF (25 ng/ml) plus CHX (4 μg/ml) for 30 min, then lysed and NEMO was immunoprecipitated (IP) and precipitates immunoblotted with anti-SUMO1 antibodies. (**d**) LS513 cells were transfected and treated as in (**c**), then lysed and RIPK1 was immunoprecipitated with RIPK1 antibody and precipitates immunoblotted with anti-K63-specific ubiquitin or RIPK1 antibodies. (**e**) LS513 and LIM2463 cells were transfected as in (**a**), and then treated with cytotoxic drugs as indicated for a further 72 h. Live cell activity in the cultures was determined by measuring ATP levels and expressed as % of cells treated with control siRNA and vehicle control, with the IC_{50} of *MUC13* siRNA and control siRNA for each drug indicated. (**a–e**) The data are representative of three independent experiments.
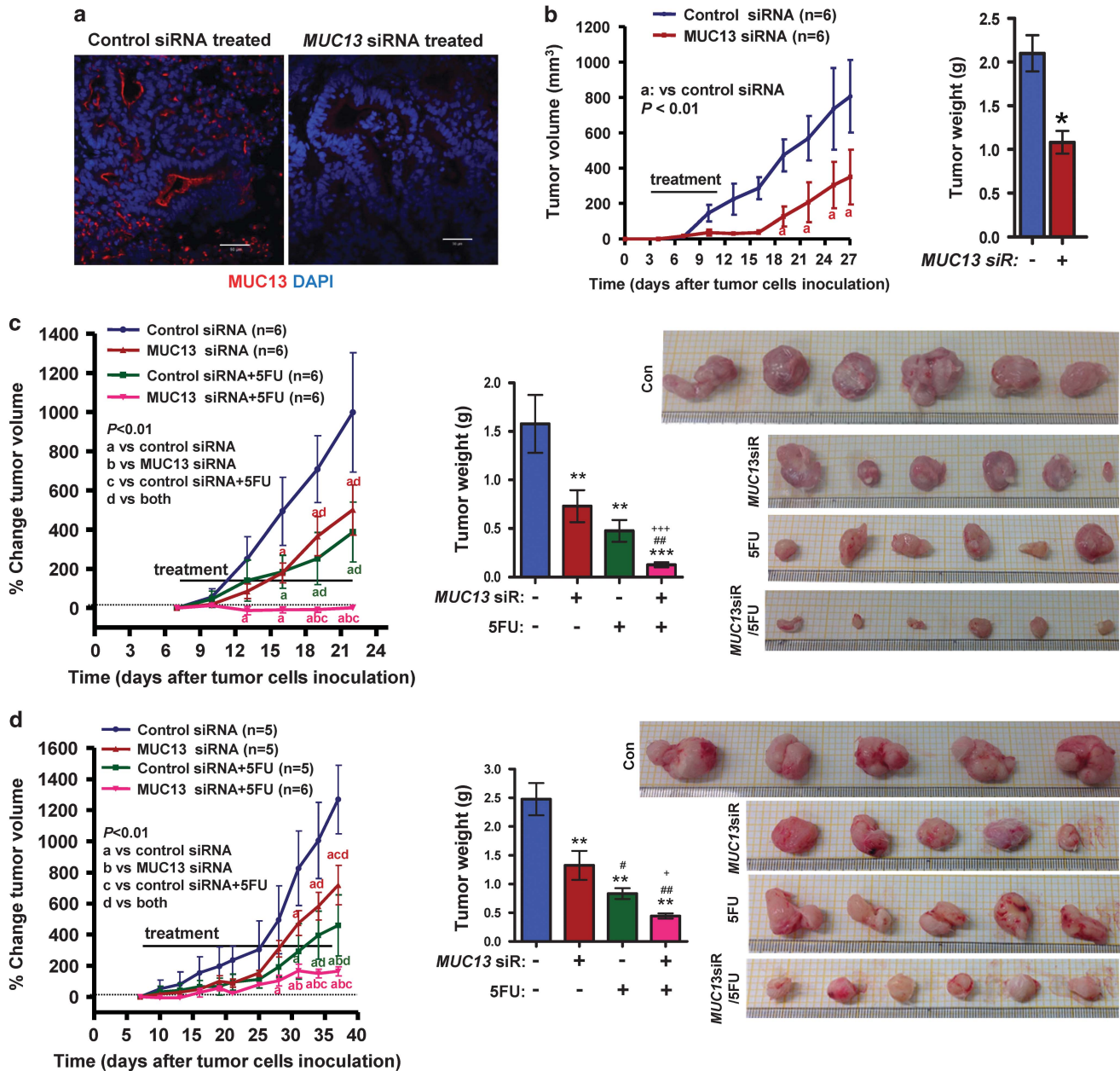
Figure 6. Combination therapy with *MUC13* siRNA liposomes and 5-fluorouracil prevents growth of colorectal cancer xenografts. (**a**, **b**) NOD/SCID gamma mice bearing subcutaneous LS513 xenografts (*n* = 6) were treated with liposomes loaded with *MUC13* or control siRNA (40 µg per mouse/i.v.) on days 3, 5, 7 and 10 after inoculation with 1×10^6 tumor cells. (**a**) Immunofluorescence staining for MUC13 in LS513 xenograft tumors from mice harvested one day following the final *MUC13* siRNA liposome treatment. Scale bar, 50 µm. (**b**) The mean tumor volume throughout the experiment and tumor weight on sampling at day 27 are shown. (**c**, **d**) NOD/SCID gamma mice bearing LS513 (**c**) and HT29 (**d**) xenografts (*n* = 5–6) were treated once mean tumor volume reached 100–200 mm³ with either liposomes loaded with *MUC13* or control siRNA (40 µg per mouse/i.v.) twice a week, 5-fluorouracil (5-FU) (50 mg/kg weekly/i.v.) or *MUC13* siRNA-loaded liposomes plus 5-FU, and tumor volume and weight measured as in (**a**) with the dissected tumors shown on the right. Data are representative of two independent experiments, mean ± s.e.m. (*n* shown in figure); two-way ANOVA with Bonferroni *post hoc* tests for tumor volume in (**b**–**d**); Mann–Whitney *U*-test for tumor weight (**b**–**d**), * vs control siRNA treatment (**b**–**d**), # vs *MUC13* siRNA treatment (**c**, **d**), + vs 5-FU/control siRNA treatment (**c**, **d**), *,#,+$P < 0.05$, **,##,++$P < 0.001$, ***,###,+++$P < 0.0001$. See Supplementary Figure S5 for white blood cell counts in the experiments in (**c**) and (**d**).

while the experimental xenograft system used with specific siRNA silencing for human *MUC13* means we can be sure the functional effects were attributable to silencing human *MUC13* in the cancer cells, we were not capable of assessing the consequences for normal tissues of *MUC13* silencing. *Muc13* knockout mice do not have any clear phenotype under normal conditions, suggesting targeting MUC13 will be unlikely to have substantial toxicity.

Although 5-FU is the mainstay approach for patients with advanced colorectal cancer and many patients will show initial

responses, recurrence and metastasis due to drug resistance remain major obstacles. Moreover, toxicity issues with 5-FU limit dose escalation and applicability. Therefore, the combination of other agents with 5-FU has been the focus of considerable investigation to improve response rates. NF-κB activity has been proposed to mediate chemotherapy resistance in colorectal cancer due to its central role in regulating multiple survival and antiapoptotic genes. Consistent with this, we observed that xenografts treated with 5-FU have increased phosphorylation of NF-κB. Importantly, we observed

a significant reduction of NF-κB activation when we combined 5-FU with *MUC13* siRNA. Moreover, blockade of NF-κB activation increased 5-FU-induced cell death in MUC13 expressing, but not MUC13-deficient, cells. The synergistic actions of *MUC13* siRNA and 5-FU may also be due to MUC13-mediated protection of CSC. In particular, we show MUC13 expression is required for enrichment
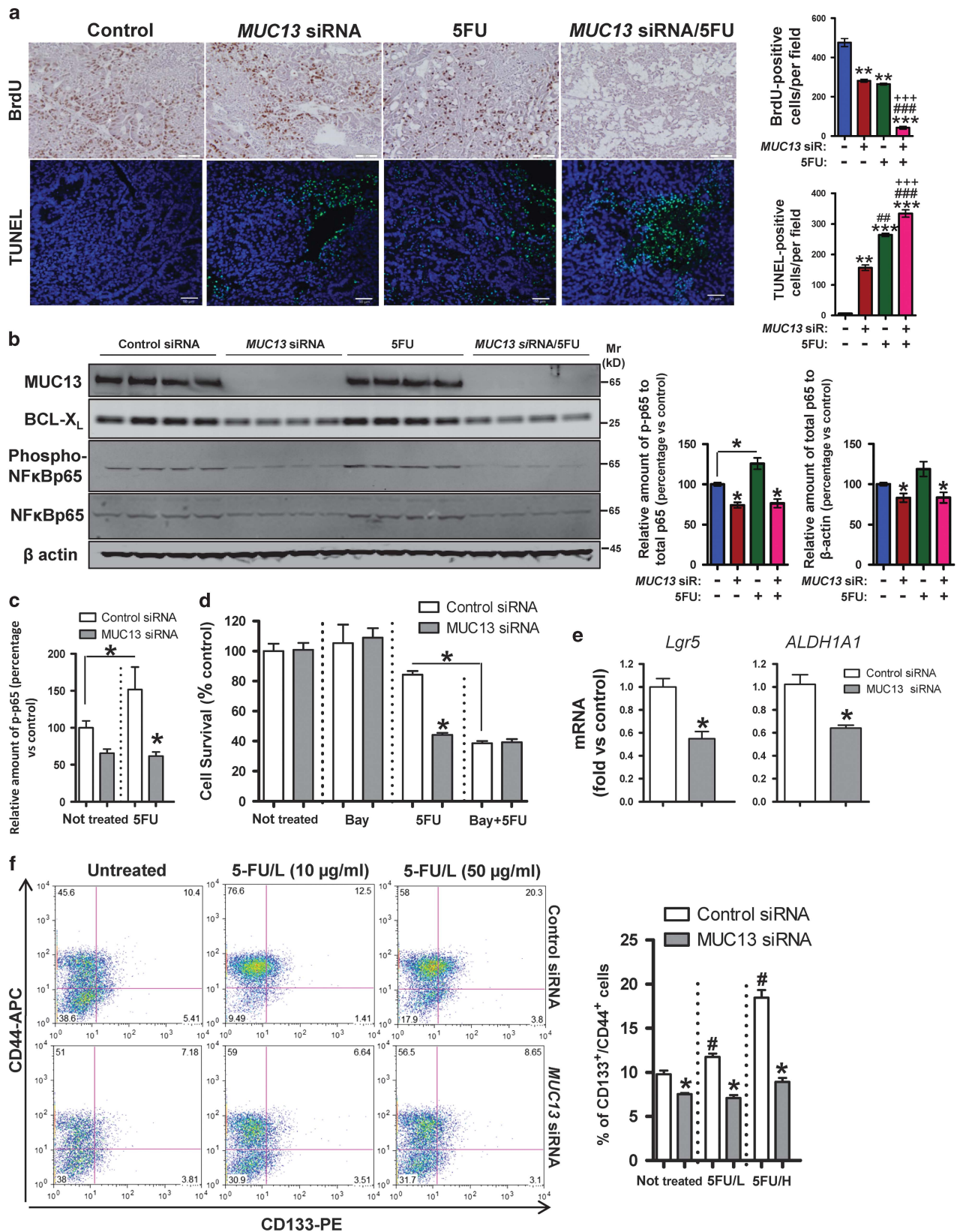
of the frequency of CD133^{+}/CD44^{+} self-renewing CSC populations after 5-FU treatment. Taken together, these results demonstrated that MUC13 promotes survival of colon cancer cells under stress via multiple mechanisms, making this mucin a potentially important new target for the treatment of advanced colorectal cancer.

Our key finding with respect to cancer therapy is that decreasing MUC13 expression in colon cancer xenografts by *MUC13* siRNA liposome treatment suppresses tumor growth and sensitizes tumors to chemotherapy. Our finding is consistent with observations that silencing *MUC1* or *MUC4* can reverse resistance to trastuzumab in HER2/ERB2-positive gastric cancers.[11,44] In summary, this report implicates MUC13 as a drugable target for colorectal cancer because MUC13 is an important driver of NF-κB-mediated survival genes. Plausibly, the same principle could be applied for other MUC13-expressing cancers. MUC13 has been shown to increase expression of the HER2/c-erbB2 growth factor receptor in ovarian and pancreatic cancers, accompanied by increased activation of downstream signaling pathways.[21,22] Enhanced growth factor expression may be downstream of the NF-κB-mediated effects we describe or may be NF-κB-independent effects of MUC13 that could also operate in colon cancer cells. Future studies should focus on defining the nature of MUC13 molecular interactions and developing small-molecule inhibitors for these interactions that could be tested as therapeutics. Targeting MUC13 reveals a novel avenue for specifically suppressing the NF-κB-mediated survival pathway in MUC13-expressing cancers including colon, ovarian, pancreatic, breast and lung cancers.

MATERIALS AND METHODS
More detailed information is described in Supplementary Materials and Methods.

CRC cell lines and clinical samples
CRC cell lines LS513, SW480 and HT29 were purchased from ATCC (Manassas, VA, USA), LIM2463 were kindly provided by Dr R Whitehead, Ludwig Institute for Cancer Research, Melbourne, Australia. The cells were propagated in RPM1-1640 (Life technologies, Carlsbad, CA, USA) with 10% heat inactivated fetal calf serum, 100 U/ml penicillin, 100 μg/ml streptomycin and 2 mM L-glutamine and all the cell lines are mycoplasma free.

Primary tumor and adjacent normal colon biopsies ($n = 58$) were obtained at colonoscopy from 29 patients with primary CRC. All patients gave informed consent for the participation in the research. This study was approved by the Mater Health Services Human Research Ethics Committee. Additionally, a high-density colon cancer tissue microarray spotted with 196 cases/200 core (#CO2001; including pathology grade) and a colon cancer progression tissue microarray spotted with 103 cases/208 cores (#CO2081) were purchased from US Biomax, Inc. (Biomax, Rockville, MD, USA). The expression of MUC13 was analyzed by immunohistochemistry with the anti-MUC13 polyclonal antibody (R20C1). The stained slides were scored blindly by a pathologist according to the value of immune reactive scores systems as following: The proportion of positive cancer cell staining was graded as follows: 0 (negative), < 25% (1+), 25–50% (2+), 50–70% (3+) and >75% (4+). The staining intensity of cancer cells was graded as weak (1+), moderate (2+) or strong (3+).

Antibodies
The antibodies used in this study were anti-BCL-X$_L$ (#2764; Cell Signaling Technology, Danvers, MA, USA), anti-BIM (#1036; Epitomics, Burlingame, CA, USA), anti-β-actin (#MAB1501; Novus Biologicals, Littleton, CO, USA), anti-MUC13 for IP and western blot analyses (#H-300; Santa Cruz Biotechnology, Dallas, TX, USA), anti-MUC13 for immunostaining (R20c1), which has been further validated through siRNA-mediated knockdown and western blotting as well as lack of immunohistochemical reactivity with intestines from Muc13 knockout mice (Supplementary Figure S6). Anti-p-NF-κBp65 (Ser536) (#3033; Cell Signaling Technology), anti-p-IκBα (Ser32) (#2859; Cell Signaling Technology), anti-lamin B (#ab16048; Abcam, Cambridge, UK), anti-total IκBα (#4814; Cell Signaling Technology), anti-cIAP1 (#7065; Cell Signaling Technology), anti-TNFR1 (#3736; Cell Signaling Technology), anti-TRAF6 (#8082; Cell Signaling Technology), anti-K63-linkage specific polyubiquitin (#5621; Cell Signaling Technology), anti-RIPK1 (#3493; Cell Signaling Technology), anti-PARP (#9542; Cell Signaling Technology).

Tumor xenograft experiments
NOD/SCID gamma mice (combined immune deficiency mutation (scid) and IL2 receptor gamma chain deficiency) were used for all studies ($n = 5$–6). Mice were sex and age matched within experiments (6–12 weeks of age). LS513 or HT29 cells were suspended in 50% matrigel and injected subcutaneously into the flanks of mice. Cages of mice were allocated to treatment groups by random draw. Treatments started either 3 days after cell inoculation or once tumors reached an average volume of ~ 100–200 mm³, liposomal *MUC13* or control siRNA (40 μg) were prepared in phosphate-buffered saline and administered twice a week by intravenous tail vein injection. Tumor volume was monitored twice a week by caliper measurements until the cessation of the experiment when tumors reached an ethically unacceptable size in any group. The person dissected the tumors was blinded to the treatment and the numbers of BrdU[+] and TUNEL^{+} cells in the LS513 tumors were blindly counted. The experiments involving mice were conducted in accordance with the Australian Code for the Care and Use of Animals for Scientific Purposes 8th edition (2013) and were approved by University of Queensland Animal Experimentation Ethics Committee.

Statistical analysis
All statistical analyses were performed using Prism v5 (Graphpad Software, La Jolla, CA, USA). Sample sizes for experiments were determined by power analyses based on the variation shown in previous experiments and predicted effect sizes considered to be of biological relevance. All replicates are true biological replicates and all statistical tests were conducted as two-sided tests. No data were excluded from any analyses. The normal distribution of data was assessed by probability plots and where a normal distribution could not be established non-parametric testing was used. The statistical test used and the sample sizes for individual analyses are provided within the figure legends.

Study approval
All the mouse experiments were approved by University of Queensland Animal Experimentation Ethics Committee (AEC no: MMRI/517/12/CCQ). The human study was approved by Mater Health Services Human Research Ethics Committee (AEC no: 1687A).
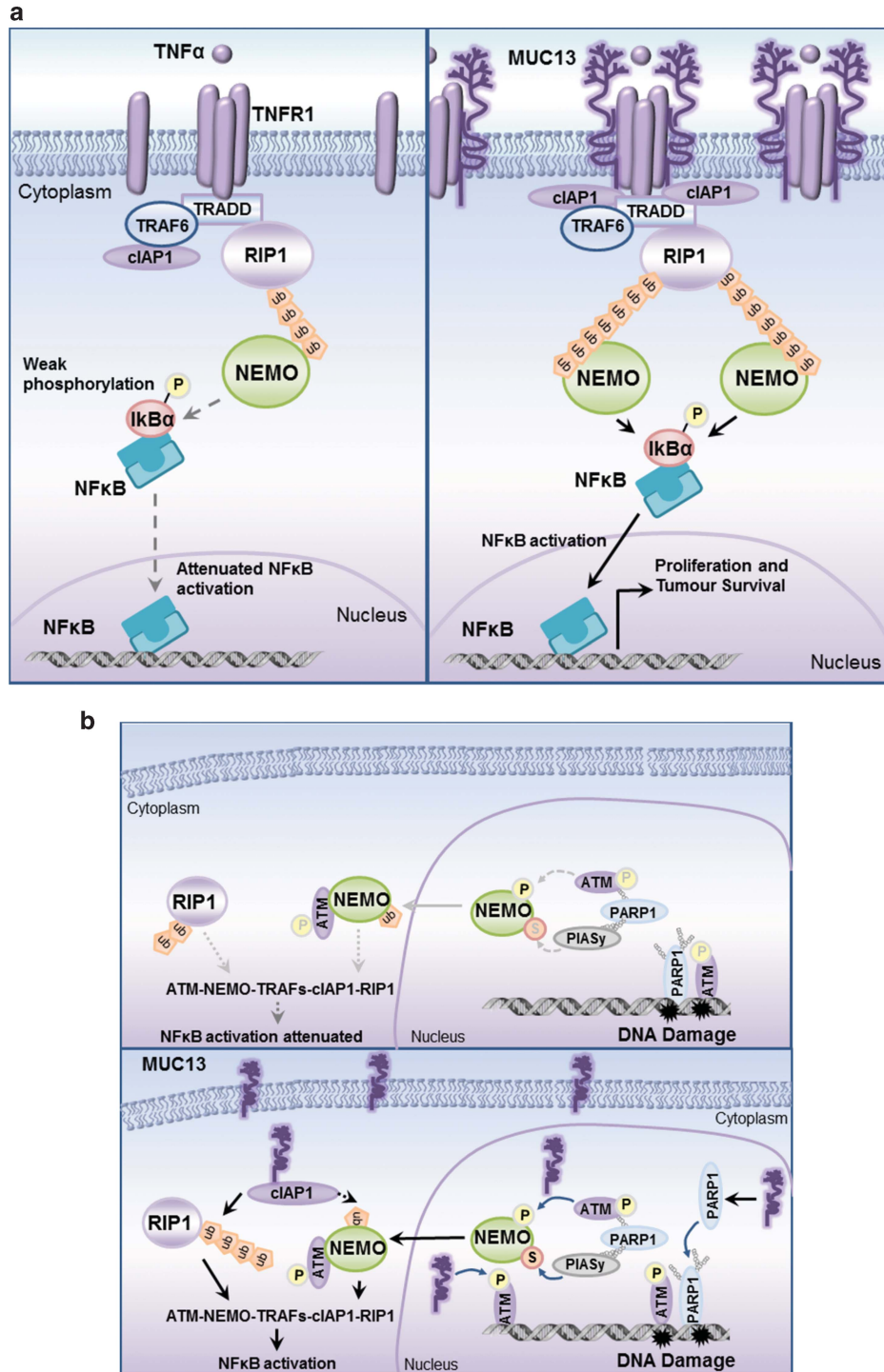
Figure 7. *MUC13* siRNA treatment suppresses 5-fluorouracil-induced NF-κB activation and enrichment of cancer stem cells and enhances the efficacy of 5-fluorouracil *in vitro* and *in vivo*. (**a**) LS513 tumor tissue from the experiment described in Figure 6c was evaluated by immunohistochemistry for BrdU-positive cells, or by fluorescent TUNEL staining and the number of stained cells per high-power field determined. Scale bar, 100 μM (BrdU) and 50 μM (TUNEL). (**c**) Immunoblot analysis with the indicated antibodies of LS513 tumor lysates from the experiment described in Figure 6c; densitometry analysis of the amount of phosphorylated NF-κB relative to total NF-κB and the total amount of NF-κB relative to β-actin is shown. (**c–f**) LS513 cells were transfected with *MUC13* or control siRNA for 48 h before treatment as described. (**c**) Cells were treated with 5-FU (50 μg/ml) for 24 h and phosphorylation of NF-κB p65 Ser536 was measured by AlphaScreen SureFire Assay and expressed as % of cells treated with control siRNA and vehicle control. (**d**) Cells were treated with Bay 11-7085 (5 μM) and/or 5-FU (5 μg/ml) for 72 h. Live cell activity in the cultures was determined by measuring ATP levels and expressed as % of cells treated with control siRNA and vehicle control. (**e**) Relative *of Lgr5 and ALDH1A1* mRNA levels (corrected for the β-actin) in otherwise untreated cells. (**f**) Representative flow cytometry profiles and bar graphs showing the percentages of CD133^{+}/CD44^{+} stem cells in LS513 cells after 24 h 5-FU treatment. A representative of three independent experiments is shown as mean ± s.e.m.; Mann–Whitney *U*-test, * vs control siRNA treatment (**a**, **b**), * vs control siRNA with the same treatment or as indicated (**c–f**), # vs *MUC13* siRNA treatment (**a**), or vs control untreated (**f**), + vs 5-FU/control siRNA treatment (**a**), *,#P < 0.05, **,##,++P < 0.001, ***,###,+++P < 0.0001.

Figure 8. Proposed mechanistic scheme of MUC13 regulating NF-κB activation, related to Figures 3–5 and Supplementary Figure S3. (**a**) Role of MUC13 in the membrane-associated TNFR complex. Connection between the proteins shows their ability to bind directly. Given that human colorectal cancers and some colorectal cancer cell lines aberrantly overexpress MUC13 while exhibiting low expression of TNFR1 (Figure 3 and Supplementary Figure S3), we propose that binding of MUC13 to TNFR1 increases clustering of the TNFR1 signaling complex, thereby amplifying the efficiency of TNF-induced signaling. In this context, MUC13 is a key to the appropriate organization at the cell membrane of the complex that forms around TNFR1. Following TNF stimulation, TNFR1 engages receptor adaptor proteins (TRADD, TRAFs and RIPK1), and MUC13 then facilitates the recruitment of the ubiquitin ligase cIAP1 to the TNF-receptor signaling complex, resulting in K63-linked ubiquitination of RIPK1. Polyubiquitylated RIPK1 provides docking sites to recruit NEMO that precedes TAK1-IKK-IκB phosphorylation and NF-κB activation. (**b**) Role for MUC13 in regulating NF-κB activation in response to genotoxins. DNA-damaging agents induce MUC13 cytoplasmic and nuclear translocation and/or retention (Figure 5a), allowing MUC13 to accumulate in the cytosol or nucleus where MUC13 promotes the phosphorylation of ATM (Figure 5b). In addition, MUC13 induces the SUMOylation of NEMO by increasing the expression of PARP1, which in turn acts as a DNA damage sensor and catalyses the formation of polyADP-ribose on target substrates, including on PARP1 itself. Auto-modified PARP1 promotes NEMO SUMOylation in the nucleus by assembling a signaling complex. Given that MUC13 interacts with cIAP1, MUC13 may recruit cIAP1 or other E3 ligases to NEMO, leading to its enhanced ubiquitination. As a consequence, ubiquitination of NEMO and activation of ATM ultimately lead to activation of IKKs and NF-κB to promote cell survival after DNA damage.

CONFLICT OF INTEREST

The authors declare no conflict of interest.

REFERENCES

1 Hanahan D, Weinberg RA. Hallmarks of cancer: the next generation. *Cell* 2011; **144**: 646–674.

2 Ni Chonghaile T, Sarosiek KA, Vo TT, Ryan JA, Tammareddi A, Moore Vdel G et al. Pretreatment mitochondrial priming correlates with clinical response to cytotoxic chemotherapy. *Science* 2011; **334**: 1129–1133.

3 McAuley JL, Linden SK, Png CW, King RM, Pennington HL, Gendler SJ et al. MUC1 cell surface mucin is a critical element of the mucosal barrier to infection. *J Clin Invest* 2007; **117**: 2313–2324.

4 Sheng YH, Hasnain SZ, Florin TH, McGuckin MA. Mucins in Ibd and colorectal cancer. *J Gastroenterol Hepatol* 2011; **27**: 28–30.

5 McGuckin MA, Linden SK, Sutton P, Florin TH. Mucin dynamics and enteric pathogens. *Nat Rev Microbiol* 2011; **9**: 265–278.

6 Jonckheere N, Skrypek N, Van Seuningen I. Mucins and tumor resistance to chemotherapeutic drugs. *Biochim Biophys Acta* 2014; **1846**: 142–151.

7 Nath S, Mukherjee P. MUC1: a multifaceted oncoprotein with a key role in cancer progression. *Trends Mol Med* 2014; **20**: 332–342.

8 Andrianifahanana M, Moniaux N, Schmied BM, Ringel J, Friess H, Hollingsworth MA et al. Mucin (MUC) gene expression in human pancreatic adenocarcinoma and chronic pancreatitis: a potential role of MUC4 as a tumor marker of diagnostic significance. *Clin Cancer Res* 2001; **7**: 4033–4040.

9 Hollingsworth MA, Strawhecker JM, Caffrey TC, Mack DR. Expression of MUC1, MUC2, MUC3 and MUC4 mucin mRNAs in human pancreatic and intestinal tumor cell lines. *Int J Cancer* 1994; **57**: 198–203.

10 McDermott KM, Crocker PR, Harris A, Burdick MD, Hinoda Y, Hayashi T et al. Overexpression of MUC1 reconfigures the binding properties of tumor cells. *Int J Cancer* 2001; **94**: 783–791.

11 Swartz MJ, Batra SK, Varshney GC, Hollingsworth MA, Yeo CJ, Cameron JL et al. MUC4 expression increases progressively in pancreatic intraepithelial neoplasia. *Am J Clin Pathol* 2002; **117**: 791–796.

12 Kufe DW. Mucins in cancer: function, prognosis and therapy. *Nat Rev Cancer* 2009; **9**: 874–885.

13 Kufe DW. MUC1-C oncoprotein as a target in breast cancer: activation of signaling pathways and therapeutic approaches. *Oncogene* 2013; **32**: 1073–1081.

14 Hollingsworth MA, Swanson BJ. Mucins in cancer: protection and control of the cell surface. *Nat Rev Cancer* 2004; **4**: 45–60.

15 Nishii Y, Yamaguchi M, Kimura Y, Hasegawa T, Aburatani H, Uchida H et al. A newly developed anti-Mucin 13 monoclonal antibody targets pancreatic ductal adenocarcinoma cells. *Int J Oncol* 2015; **46**: 1781–1787.

16 Shimamura T, Ito H, Shibahara J, Watanabe A, Hippo Y, Taniguchi H et al. Overexpression of MUC13 is associated with intestinal-type gastric cancer. *Cancer Sci* 2005; **96**: 265–273.

17 Walsh MD, Young JP, Leggett BA, Williams SH, Jass JR, McGuckin MA. The MUC13 cell surface mucin is highly expressed by human colorectal carcinomas. *Hum Pathol* 2007; **38**: 883–892.

18 Gupta BK, Maher DM, Ebeling MC, Stephenson PD, Puumala SE, Koch MR et al. Functions and regulation of MUC13 mucin in colon cancer cells. *J Gastroenterol* 2014; **49**: 1378–1391.

19 Gupta BK, Maher DM, Ebeling MC, Sundram V, Koch MD, Lynch DW et al. Increased expression and aberrant localization of mucin 13 in metastatic colon cancer. *J Histochem Cytochem* 2012; **60**: 822–831.

20 Khan S, Ebeling MC, Zaman MS, Sikander M, Yallapu MM, Chauhan N et al. MicroRNA-145 targets MUC13 and suppresses growth and invasion of pancreatic cancer. *Oncotarget* 2014; **5**: 7599–7609.

21 Chauhan SC, Ebeling MC, Maher DM, Koch MD, Watanabe A, Aburatani H et al. MUC13 mucin augments pancreatic tumorigenesis. *Mol Cancer Ther* 2012; **11**: 24–33.

22 Chauhan SC, Vannatta K, Ebeling MC, Vinayek N, Watanabe A, Pandey KK et al. Expression and functions of transmembrane mucin MUC13 in ovarian cancer. *Cancer Res* 2009; **69**: 765–774.

23 Williams SJ, Wreschner DH, Tran M, Eyre HJ, Sutherland GR, McGuckin MA. Muc13, a novel human cell surface mucin expressed by epithelial and hemopoietic cells. *J Biol Chem* 2001; **276**: 18327–18336.

24 Linden SK, Sutton P, Karlsson NG, Korolik V, McGuckin MA. Mucins in the mucosal barrier to infection. *Mucosal Immunol* 2008; **1**: 183–197.

25 Sheng YH, Lourie R, Linden SK, Jeffery PL, Roche D, Tran TV et al. The MUC13 cell-surface mucin protects against intestinal inflammation by inhibiting epithelial cell apoptosis. *Gut* 2011; **60**: 1661–1670.

26 Meier P, Vousden KH. Lucifer's labyrinth—ten years of path finding in cell death. *Mol cell* 2007; **28**: 746–754.

27 Dolcet X, Llobet D, Pallares J, Matias-Guiu X. NF-kB in development and progression of human cancer. *Virchows Arch* 2005; **446**: 475–482.

28 Baldwin AS. Control of oncogenesis and cancer therapy resistance by the transcription factor NF-kappaB. *J Clin Invest* 2001; **107**: 241–246.

29 Janssens S, Tinel A, Lippens S, Tschopp J. PIDD mediates NF-kappaB activation in response to DNA damage. *Cell* 2005; **123**: 1079–1092.

30 Tsujimoto Y. Role of Bcl-2 family proteins in apoptosis: apoptosomes or mitochondria? *Genes Cells* 1998; **3**: 697–707.

31 Lin A, Karin M. NF-kappaB in cancer: a marked target. *Semin Cancer biology* 2003; **13**: 107–114.

32 Sheng YH, Triyana S, Wang R, Das I, Gerloff K, Florin TH et al. MUC1 and MUC13 differentially regulate epithelial inflammation in response to inflammatory and infectious stimuli. *Mucosal Immunol* 2013; **6**: 557–568.

33 Ahmad R, Raina D, Joshi MD, Kawano T, Ren J, Kharbanda S, Kufe D. MUC1-C oncoprotein functions as a direct activator of the nuclear factor-kappaB p65 transcription factor. *Cancer Res* 2009; **69**: 7013–7021.

34 Ahmad R, Raina D, Trivedi V, Ren J, Rajabi H, Kharbanda S et al. MUC1 oncoprotein activates the IkappaB kinase beta complex and constitutive NF-kappaB signalling. *Nat Cell Biol* 2007; **9**: 1419–1427.

35 Silke J, Vaux D. *IAPs and Necroptotic Cell Death*. Humana Press Inc: New York, NY, USA, 2014, pp 57–77.

36 Iwai K. Diverse ubiquitin signaling in NF-kappaB activation. *Trends Cell Biol* 2012; **22**: 355–364.

37 Li N, Banin S, Ouyang H, Li GC, Courtois G, Shiloh Y et al. ATM is required for IkappaB kinase (IKKk) activation in response to DNA double strand breaks. *J Biol Chem* 2001; **276**: 8898–8903.

38 Wu SY, Putral LN, Liang M, Chang HI, Davies NM, McMillan NA. Development of a novel method for formulating stable siRNA-loaded lipid particles for in vivo use. *Pharm Res* 2009; **26**: 512–522.

39 Li F, Sethi G. Targeting transcription factor NF-kappaB to overcome chemoresistance and radioresistance in cancer therapy. *Biochim Biophys Acta* 2010; **1805**: 167–180.

40 Jordan CT, Guzman ML, Noble M. Cancer stem cells. *N Engl J Med* 2006; **355**: 1253–1261.

41 McCool KW, Miyamoto S. DNA damage-dependent NF-kappaB activation: NEMO turns nuclear signaling inside out. *Immunol Rev* 2012; **246**: 311–326.

42 Breccia M, Alimena G. NF-kappaB as a potential therapeutic target in myelodysplastic syndromes and acute myeloid leukemia. *Expert Opin Ther Targets* 2010; **14**: 1157–1176.

43 DiDonato JA, Mercurio F, Karin M. NF-kappaB and the link between inflammation and cancer. *Immunol Rev* 2012; **246**: 379–400.

44 Deng M, Jing DD, Meng XJ. Effect of MUC1 siRNA on drug resistance of gastric cancer cells to trastuzumab. *Asian Pac J Cancer Prev* 2013; **14**: 127–131.